Airway antibodies wane rapidly after COVID-19 but B cell memory is generated across disease severity

Alberto Cagigi[1], Meng Yu[1], Sara Falck-Jones[1], Sindhu Vangeti[1], Björn Österberg[1], Eric Åhlberg[1], Lida Azizmohammadi[1], Ryan Falck-Jones[2,3], Pia C Gubisch[1], Mert Ödemis[1], Farangies Ghafoor[1], Klara Lenart[1], Max Bell[2,3], Niclas Johansson[4,5], Jan Albert[6,7], Jörgen Sälde[8], Deleah Pettie[9,10], Michael Murphy[9,10], Lauren Carter[9,10], Neil P King[9,10], Sebastian Ols[1], Anna Färnert[4,5], Karin Loré[1*] and Anna Smed-Sörensen[1*]

[1]Division of Immunology and Allergy, Department of Medicine Solna, Karolinska Institutet, Karolinska University Hospital, Stockholm, Sweden. [2]Department of Physiology and Pharmacology, Karolinska Institutet, Stockholm, Sweden. [3]Department of Perioperative Medicine and Intensive Care, Karolinska University Hospital, Stockholm, Sweden. [4]Division of Infectious Diseases, Department of Medicine Solna, Center for Molecular Medicine, Karolinska Institutet, Sweden. [5]Department of Infectious Diseases, Karolinska University Hospital Solna, Stockholm, Sweden. [6]Department of Microbiology, Tumor and Cell Biology, Karolinska Institutet, Stockholm, Sweden. [7]Clinical Microbiology, Karolinska University Hospital Solna, Stockholm, Sweden. [8]Närakut SLSO, Karolinska University Hospital Solna, Stockholm, Sweden. [9]Department of Biochemistry, University of Washington, Seattle, WA 98195, United States. [10]Institute for Protein Design, University of Washington, Seattle, WA 98195, United States. [*]Equal contribution.

Correspondence to:
Karin Loré and Anna Smed-Sörensen, Division of Immunology and Allergy, Department of Medicine Solna, Karolinska Institutet, Visionsgatan 4, BioClinicum J7:30, Karolinska University Hospital, 171 64 Stockholm, Sweden.
e-mail addresses: karin.lore@ki.se; anna.smed.sorensen@ki.se

Conflict of interest statement
The authors have declared that no conflict of interest exists.

Summary

COVID-19 severity determines the level of systemic and airway IgG and IgA but while IgG are maintained in plasma during convalescence, antibodies wane rapidly in the airways. However, comparable levels of antigen-specific memory B cells are generated across disease severity.

Abstract

Understanding immune responses following SARS-CoV-2 infection in relation to COVID-19 severity is critical for predicting the effects of long-term immunological memory on viral spread. Here we longitudinally assessed systemic and airway immune responses against SARS-CoV-2 in a well-characterized cohort of 147 infected individuals representing the full spectrum of COVID-19 severity; from asymptomatic infection to fatal disease. High systemic and airway antibody responses were elicited in patients with moderate to severe disease, and while systemic IgG levels were maintained after acute disease, airway IgG and IgA declined significantly. In contrast, individuals with mild symptoms showed significantly lower antibody responses but their levels of antigen-specific memory B cells were comparable with those observed in patients with moderate to severe disease. This suggests that antibodies in the airways may not be maintained at levels that prevent local virus entry upon re-exposure and therefore protection via activation of the memory B cell pool is critical.

Introduction

Severe acute respiratory syndrome coronavirus 2 (SARS-CoV-2) infection that causes coronavirus disease 2019 (COVID-19) can present with a wide range of disease severity from asymptomatic to fatal. Individuals of advanced age and/or those with comorbidities are overrepresented among patients who develop severe disease (Zaki et al., 2020). However, the majority of SARS-CoV-2 infected individuals experience asymptomatic infection or only mild disease (Moghadas et al., 2020). Understanding immune responses following SARS-CoV-2 infection in relation to COVID-19 severity is critical for predicting long-term immunological memory and the potential risk for re-infection or virus spread. Whether patients with different disease severities generate similar protective immunity is still unknown. Here we present longitudinal data on virus-specific systemic and airway antibody and B cell memory responses generated in a clinically well-characterized cohort of individuals with SARS-CoV-2 infection (n=147) representing the full spectrum of COVID-19 severity ranging from asymptomatic infection to fatal disease.

Results and discussion

Individuals were sampled during disease and convalescence with longitudinal, donor-matched blood and airway samples. The levels of systemic and airway antibody responses as well as the generation of SARS-CoV-2-specific memory B cells were measured. Plasma, peripheral blood mononuclear cells (PBMC), nostril swabs (NSW) and nasopharyngeal aspirates (NPA) were collected across all disease severities whereas endotracheal aspirates (ETA) were collected only from intubated patients receiving intensive care (Figure 1A). Disease severity was assessed daily, using a seven-point scale derived from the respiratory domain of the sequential organ failure assessment (SOFA) score (Grissom et al., 2010; Vincent et al., 1996), with additional levels for non-admitted mild cases (1) and fatal cases (7). Patients were later grouped based on peak disease severity (PDS) (Table 1). In addition, pre-pandemic healthy controls (PPHC) (n=30) as well as individuals who experienced influenza-like symptoms and were possibly exposed to SARS-Cov-2 but had a negative diagnostic PCR (PCR-) (n=9) were sampled in the same way and included as controls.

We first assessed systemic IgG and IgA responses at the time of study inclusion that ranged between 0-54 days from onset of symptoms; median 16 days. Generally, patients with the highest peak disease severity score were included in the study after they had already been hospitalized for a number of days (Figure 1B) (Falck-Jones et al., 2020). Therefore, these individuals were sampled longer after symptom onset as compared with individuals with mild disease resulting in a large time frame of study inclusion with respect to symptom onset (Table 1). For simplicity, this sampling period/study inclusion is referred to as the “acute” phase. Samples collected at the first follow-up visit (46-168 days; median 108 days) are referred to as the “convalescent” phase. Time of convalescent from acute sampling ranged based on individual patient recovery and their disease severity (33-159 days; median 90 days). Plasma IgG and IgA against the SARS-CoV-2 nucleocapsid (N) and spike (S) proteins as well as the receptor binding domain (RBD) (Walls et al., 2020; Wrapp et al., 2020) of the S protein were measured by ELISA. Antibody responses against the internal N protein have been shown to be elevated in deceased individuals but whether these antibodies contribute

to disease severity is unknown (Atyeo et al., 2020; Guthmiller et al., 2020). In contrast, antibody responses against the viral surface protein S and, in particular, against the RBD result in virus neutralization (Piccoli et al., 2020). Responses against the RBD are thus likely necessary for protection from re-infection or prevention of symptomatic disease.

In line with previous reports (Atyeo et al., 2020; Gaebler et al., 2020; Gudbjartsson et al., 2020; Guthmiller et al., 2020; Zhao et al., 2020), plasma IgG and IgA responses against N, S and RBD were robust in acute disease in the majority of individuals with moderate to severe disease while they were substantially lower in individuals with mild disease (Figure 2A). However, in our cohort, this might also partially be due to earlier study inclusion of patients with mild symptoms (median days from onset of symptoms 11 as compared with 13 and 21.5 in the moderate and severe groups respectively, and 13 in the fatal group) (Table 1). In fact, while plasma IgG levels remained high in the patients with moderate to severe disease in the convalescent phase, levels had increased in the individuals with mild disease and all had seroconverted (Figure 2A). In contrast, IgA levels from the acute phase, against all antigens, waned substantially during convalescence in most patients (Figure 2A). While the levels of IgG against the RBD (Figure 2B), as well as against N and S (Figure S1A), exhibited a positive correlation with days from onset of symptoms during the acute phase, this was less pronounced for IgA levels. Furthermore, patients with mild disease displayed lower levels of plasma IgG against RBD as compared with more severe patients, also when samples were taken after similar duration of symptoms (Figure 2A-B and Figure S1B). Altogether, these data confirm that the generation of IgA likely precede that of IgG. Earlier reports of individuals with asymptomatic infection or mild disease also showed robust early IgA responses (Cervia et al., 2020; Staines et al., 2020; Sterlin et al., 2020).

Comparable to another study (Hansen et al., 2020), the levels of both plasma IgG and IgA against all antigens tested, during both acute disease and convalescence, were significantly higher in patients with more severe disease compared to mild, both when comparing disease severity at time of study inclusion and initial sampling as well as when grouping the patients based on their peak disease severity (Figure S2A). When comparing antibody levels between disease severity groups based on when patients were sampled after disease onset, patients with moderate or severe disease on average tended to have higher antibodies compared to those with mild disease already during the first week of symptom onset and were more pronounced after 2, 3 and >3 weeks of symptom onset (Figure S1B). However, these differences were not statistically significant in our cohort, probably due to uneven inclusion over time in the different disease severity groups. In our cohort, the difference in antibody titers over time was further supported by the fact that the patients with moderate/severe disease, and even fatal outcome, for whom we initially observed low IgG titers against RBD, had an early study inclusion (on average 13 days from onset of symptoms); but showed significantly higher titers later during the acute phase (on average 19 days) (Figure 2C-D). Similar kinetics of anti-RBD responses have previously been noted in different patient cohorts (Lynch et al., 2020; Robbiani et al., 2020; Rydyznski Moderbacher et al., 2020).

As the respiratory tract is the initial site of viral infection and replication, we next measured the levels of IgG and IgA in the upper and lower airways and compared with levels in plasma at matched time points. Due to limited sample volumes, we focused our analyses on IgG and

IgA responses against the RBD since these responses are likely most critical for virus neutralization. We found that RBD-specific antibodies could be readily detected in NSW and NPA during the acute phase in several patients across all disease severities (Figure 3A and B). In agreement with our observations in plasma, antibody levels in the upper respiratory tract were higher in patients with moderate or severe disease as compared with individuals with mild disease. Both IgG and IgA levels declined significantly in the convalescent phase, with IgG declining to almost undetectable levels (Figure 3A and B). This demonstrates that airway antibody levels wane much faster than those in plasma during convalescence. Low but detectable levels of antibodies to SARS-CoV-2 have previously been reported also in saliva during convalescence (Isho et al., 2020). However, whether these low antibody levels at mucosal sites will be sufficient for protection is not known. We found that RBD-specific IgG and IgA levels in the respiratory tract correlated well with those in plasma during the acute phase but to a lesser extent during convalescence (Figure 3C and Figure S2B). When comparing donor-matched NSW, NPA and ETA collected at the same time point during acute disease from intubated patients, significantly higher levels of IgA against the RBD were found in NPA as compared with NSW and ETA (Figure 3D). While this could be partially influenced by differences in sampling method and sample volume, these data suggest that antibody abundance and possibly virus neutralization via IgA differs along the respiratory tract and may be more pronounced in the nasopharynx compared to the lower airways. Hence, nasopharynx antibodies (both IgG and IgA) showed a strong correlation with plasma antibody responses (Figure 3D and Figure S2B). We also assessed the presence of B cells in the respiratory tract of COVID-19 patients by analyzing the lymphocytes that could be retrieved from NPA and ETA as compared with NPA from three additional healthy controls (HC). Lymphocyte frequencies were lower in both NPA and ETA from several COVID-19 patients as compared with NPA from HC. The proportion of B cells of lymphocytes was similar in NPA from HC and COVID-19 patients. However, the proportion of B cells in ETA of COVID-19 patients was lower compared to NPA, which possibly contributes to the higher antibody levels at this site (Figure 4A and B).

Altogether, the data presented so far confirm that moderate and severe COVID-19 result in high levels of circulating antibodies and show that despite IgG being well-maintained during convalescence, antibody levels in the airways decline significantly after the acute phase. Generally, antibodies present in circulation and at local sites are the result of secretion from short-lived plasmablasts and/or terminally differentiated plasma cells in the bone marrow or mucosal sites (Zielinski et al., 2011). The response to a secondary infection once antibody titers have waned below protective levels mostly relies on the presence of resting antigen-specific memory B cells that are rapidly activated upon antigen re-exposure (Zielinski et al., 2011). We therefore investigated the induction and maintenance of antigen-specific memory B cells similar to other studies (Dan et al., 2020; Juno et al., 2020; Rodda et al., 2020). We focused on the direct comparison between individuals with mild disease and patients with moderate/severe disease, along with individuals who had reported mild influenza-like symptoms but were SARS-CoV-2 PCR-. Patients with moderate/severe disease who had high circulating IgG and IgA levels were specifically selected for the analysis to be able to compare the opposite ends of the COVID-19 disease spectrum. Donor-matched PBMC from acute disease and convalescence were analyzed side-by-side using fluorescently labelled S and RBD probes to detect antigen-specific B cells (Dan et al., 2020; Juno et al., 2020; Rodda et al., 2020). Patients with moderate/severe disease had switched memory B

cells specific to S in the acute phase and the memory B cell pool had further expanded in the convalescent phase (ranging from 0.009 to 1.35%; mean 0.42% during convalescence) (Figure 4C-F). Individuals with mild disease showed lower memory B cells during acute disease than the patients with moderate/severe disease, but the levels had increased by the time of convalescent sampling (ranging from 0.17% to 0.64%; mean 0.35% during convalescence) and were comparable between the groups (Figure 4E and F). Further phenotyping of the S-specific memory B cells indicated that the majority of these cells may be specific for epitopes on S outside of the RBD (Figure 4D). However, it is possible that binding of B cells to RBD could be underestimated as RBD is also present in the S protein. S-specific memory B cells in the circulation were predominantly IgG+, rather than IgA+ (Figure 4D). Low frequencies of S and RBD-specific memory B cells were observed in the PCR- individuals. However, these were not significantly different from the levels observed in PPHC (Figure 4C and E). Collectively, since the majority of individuals infected with SARS-CoV-2 are either asymptomatic or experience only mild COVID-19 symptoms (Moghadas et al., 2020), the possibility of generating antigen-specific memory B cells without experiencing severe disease, would be very important in the prospect of establishing potential immunity at the population level.

In summary, here we show that COVID-19 disease severity not only determines the magnitude of systemic but also airway antibody levels with efficient generation of virus-specific memory B cells against SARS-CoV-2 also occurring upon mild disease. While plasma IgG levels were generally well detectable at convalescence in all groups, there was a significant decline in airway antibodies after the clearance of infection. This suggests that antibodies in the airways may not be maintained at levels that prevent local virus entry upon re-exposure. However, our data indicate that the majority of infected individuals have the ability to generate anamnestic responses via the memory B cell pool. Speculatively, the antibodies and memory B cell pool may play a role for protection or mitigation of disease severity in case of re-infection. Whether sufficient number of memory B cells will be maintained long-term and to what extent they will prevent the spread of SARS-CoV-2 at the population level remain to be understood. This is critical knowledge to acquire in the near future to evaluate together with the memory B cell response generated after the introduction of SARS-CoV-2 vaccination. Ultimately, the requirements for establishment of long-term protection and immunity will need to be determined.

Materials and methods

Study design, patient enrollment and sample collection

One hundred and forty-seven (147) PCR-confirmed SARS-CoV-2 infected patients were enrolled at the Karolinska University Hospital and Haga Outpatient Clinic (Haga Närakut), Stockholm, Sweden during March-May 2020 (acute phase) in a time that ranged from 0 to 54 days from onset of symptoms as self-reported by individual patients; and during April-September 2020 (convalescence) in a time that ranged from 46 to 168 days continuing from the previous counts. Patients were enrolled at various settings, ranging from primary to intensive care. In order to recruit asymptomatic and mild cases, household contacts of COVID-19 patients were screened with PCR and enrolled if positive. A small subset of these individuals who experienced influenza-like symptoms and were possibly exposed to SARS-

Cov-2 but had a negative diagnostic PCR (PCR-) (n=9 of whom 3 were household contacts of confirmed patients with 1 experiencing fever, and 6 were included based on suspected infection with 4 experiencing fever) were sampled in the same way and included as controls alongside with 30 pre-pandemic healthy control samples (PPHC) from 2016-2018.

Respiratory failure was categorized daily according to the respiratory domain of the Sequential Organ Failure Assessment score (SOFA)(Vincent et al., 1996). The modified SOFA score (mSOFA) was calculated when arterial partial pressure of oxygen (PaO_2) was not available. In this case peripheral transcutaneous hemoglobin saturation (SpO_2) was used instead (Grissom et al., 2010). Estimation of the fraction of inspired oxygen (FiO_2) based on O_2 flow was calculated as per the Swedish Intensive Care register definition (Intensivvårdsregistret, 2018). Patients were categorized based on the peak respiratory SOFA or mSOFA value with the 5-point respiratory SOFA score being extended with additional levels to include and distinguish admitted asymptomatic and non-admitted/admitted mild cases and to include fatal outcome added as a seventh level. Ten (10) patients with fatal outcome had peak disease severity score 6 prior to death and 2 patients had scores of 4 and 5. For convenience, the resulting 7-point composite peak disease severity (PDS) was condensed into a broader classification consisting of mild (1-2), moderate (3-4), severe (5-6), and fatal (7). Demographics and additional data were collected from medical records, including clinical history and risk factors such as BMI and co-morbidities. Total burden of comorbidities was assessed using the Charlson co-morbidity index (CCI) (Charlson et al., 1987) (Table 1). Additional clinical information on this patient cohort including the modulation of disease from time to study inclusion to peak severity can be found in Falck-Jones et al (Falck-Jones et al., 2020).

Blood was collected in EDTA-containing tubes from all patients except those admitted to the intensive care unit (ICU) for whom blood was pooled from heparin-coated blood gas syringes discarded in the last 12 hours. For some ICU patients, additional venous blood was also collected in EDTA tubes. Nostril swabs (NSW) and nasopharyngeal aspirates (NPA) were collected from the majority of the patients whereas endotracheal aspirates (ETA) were only collected from patients with mechanical ventilation intubated in the ICU. Admitted patients were sampled during acute disease at up to four timepoints and ICU patient material was collected up at to ten timepoints. For this study, unless otherwise stated, the measurements referring to acute disease were performed with samples collected at the time of study inclusion and during convalescence when patients returned for a follow-up visit.

The study was approved by the Swedish Ethical Review Authority, and performed according to the Declaration of Helsinki. Written informed consent was obtained from all patients and controls. For sedated patients, the denoted primary contact was contacted and asked about the presumed will of the patient and to give initial oral and subsequently signed written consent. When applicable retrospective written consent was obtained from patients with non-fatal outcomes.

Enzyme-linked immunosorbent assay (ELISA)

The presence of IgG or IgA binding against the SARS-Cov-2 Nucleocapsid (N) and Spike (S) trimer or the Receptor Binding Domain (RBD) monomer (Walls et al., 2020) in plasma and airway samples was assessed by enzyme-linked immunosorbent assay (ELISA). Recombinant

proteins were received through the global health-vaccine accelerator platforms (GH-VAP) funded by the Bill & Melinda Gates Foundation. Briefly, 96-half well plates were coated with 50ng/well of the respective protein. Plates were incubated with a selected duplicate dilution that did not provide background noise against ovalbumin used as a negative control (data not shown) (i.e. 1:20 for plasma samples, 1:2 for NSW and NPA, and 1:5 for ETA in 5% milk/PBS buffer). Duplicate 7-point serial dilutions were initially performed for measuring plasma IgG against RBD during acute disease and the half maximal effective concentration (EC_{50}) was calculated using GraphPad Prism 9. However, since for several samples with low antibody concentration (mostly from the asymptomatic/mild category) the EC_{50} was below the highest dilution used (of 1:20) and therefore below the limit of detection (Figure S3A), the maximal optical density (OD) at 1:20 dilution was used instead for this and for all the other measurements subsequently performed. The relation with maximal OD and EC_{50} was also verified in a subset of patients with high IgG and IgA against S (Figure S3B). Detection was performed with mouse and goat anti-human IgG or IgA HRP-conjugated secondary antibodies (clone G18-145 from BD Biosciences and polyclonal from ThermoFisher, respectively) followed by incubation with TMB substrate (BioLegend) which was stopped with a 1M solution of sulfuric acid. Blocking with 5% milk/PBS buffer and washing with 0.1% Tween-20/PBS buffer were performed between each step. Absorbance was read at 450nm and background correction at 550nm using an ELISA reader. Data were reported as maximal absorbance i.e. OD, as stated above, and plotted using GraphPad Prism 9. All of the antibody measurements in plasma and respiratory samples from SARS-CoV-2 patients were run alongside with samples from two different control groups as described above. Interestingly, low but readily detectable IgA reactivity against S was detected in the pre-pandemic healthy controls and in the PCR- individuals (Figure S3C). After having verified the specificity and sensitivity of our ELISA assay for IgA detection with limiting sample dilutions (Figure S3D), we hypothesize that this might be due to cross-reactivity on the shared portions of the S protein between SARS-CoV-2 and other common cold coronaviruses. Reports have shown that cross-reactivity between coronaviruses exists (Grifoni et al., 2020; Song et al., 2020).

Flow cytometry

Staining of cells from airway samples was performed fresh. Briefly, samples were centrifuged at 400 g for 5 min at room temperature and cells were washed with sterile PBS. Mucus was removed using a 70 μm cell strainer and cells were subsequently stained with the appropriate combination of fluorescently labelled monoclonal antibodies as illustrated in Figure 4A. Staining of PBMC was performed on previously cryopreserved samples. The appropriate combination of fluorescently labelled monoclonal antibodies binding to different cell surface markers and with fluorescently labelled S and RBD proteins used as probes for antigen-specific B cells is illustrated in Figure 4C. Probes were prepared from biotinylated proteins using a 4:1 molar ratio (protein:fluorochrome-labelled streptavidin) considering the molecular weight of protein monomers and of the streptavidin only. The probes were prepared using streptavidin conjugated to PE and APC for S and with BV421 for the RBD. The gating strategy for the identification of antigen-specific memory B cells is shown in Figure 2d. Briefly, after identification of lymphocytes in single suspension, live B cells, (i.e. cells not expressing CD3/,CD14/CD16/CD56) were gated. From this gate, B cells were further isolated by expression of CD19 and CD20 and then switched memory B cells were identified as IgD-IgM-. From these, S-specific switched memory B cells were identified by binding to both S protein probes. Further characterization was then carried out by

analyzing IgG expression (IgA+ switched memory B cells are assumed to mirror IgD-IgM-IgG- B cells) and fluorescently labelled RBD. Stained cells from airway samples were acquired using a BD LSRFortessa while stained PBMC were acquired using a BD FACSAria Fusion both interfaced with the BD FACSDiva Software. Results were analyzed using BD FlowJo version 10.

Statistical analyses

All statistical analyses were performed using GraphPad Prism 9. Spearman correlation was used to assess the interdependence of 2 different non-categorical parameters across individuals whereas Wilcoxon matched-pairs signed rank or Mann–Whitney U tests as appropriate, were used to assess differences or similarities for one single parameter between 2 different groups. Kruskal -Wallis with Dunn's multiple comparisons test was used when assessing comparison between multiple groups.

Author contributions

Experimental study design: A.C., Ka.L. and A.S-S. Clinical concept design: A.S-S., M.B., N.J., J.A., J.S. and A.F. Acquisition and sample processing: M.Y., S. F-J., S.V., B.Ö., E.Å., L.A., R.F-J., M.Ö. and F.G. Generation of data: A.C., M.Y., S. F-J., S.V. and P.C.G. Provision of custom reagents: D.P., M.M., L.C., and N.P.K. Analysis and interpretation of data: A.C., Ka.L. and A.S-S. Critical revision of the manuscript: all authors. Statistical analysis: A.C., K.L. and S.O. Ka.L. and A.S-S. contributed equally to the study.

Acknowledgments

We thank the patients and healthy volunteers who have contributed to this study. We would also like to thank medical students and hospital staff for assistance with patient sampling and collection of clinical data, the Biomedicum BSL3 core facility, Karolinska Institutet and Fredrika Hellgren for assistance with English editing. This work was supported by grants from the Swedish Research Council, the Swedish Heart-Lung Foundation, the Bill & Melinda Gates Foundation, the Knut and Alice Wallenberg Foundation through SciLifeLab and Karolinska Institutet.

372 **References**
373
374 Atyeo, C., S. Fischinger, T. Zohar, M.D. Slein, J. Burke, C. Loos, D.J. McCulloch, K.L. Newman,
375 C. Wolf, J. Yu, K. Shuey, J. Feldman, B.M. Hauser, T. Caradonna, A.G. Schmidt, T.J.
376 Suscovich, C. Linde, Y. Cai, D. Barouch, E.T. Ryan, R.C. Charles, D. Lauffenburger, H.
377 Chu, and G. Alter. 2020. Distinct Early Serological Signatures Track with SARS-CoV-2
378 Survival. *Immunity* 53:524-532 e524.
379 Cervia, C., J. Nilsson, Y. Zurbuchen, A. Valaperti, J. Schreiner, A. Wolfensberger, M.E. Raeber,
380 S. Adamo, M. Emmenegger, S. Hasler, P.P. Bosshard, E.D. Cecco, E. Bächli, A. Rudiger,
381 M. Stüssi-Helbling, L.C. Huber, A.S. Zinkernagel, D.J. Schaer, A. Aguzzi, U. Held, E.
382 Probst-Müller, S.K. Rampini, and O. Boyman. 2020. Systemic and mucosal antibody
383 secretion specific to SARS-CoV-2 during mild versus severe COVID-19. *bioRxiv*
384 2020.2005.2021.108308.
385 Charlson, M.E., P. Pompei, K.L. Ales, and C.R. MacKenzie. 1987. A new method of classifying
386 prognostic comorbidity in longitudinal studies: development and validation. *J Chronic*
387 *Dis* 40:373-383.
388 Dan, J.M., J. Mateus, Y. Kato, K.M. Hastie, C.E. Faliti, S.I. Ramirez, A. Frazier, E.D. Yu, A.
389 Grifoni, S.A. Rawlings, B. Peters, F. Krammer, V. Simon, E.O. Saphire, D.M. Smith, D.
390 Weiskopf, A. Sette, and S. Crotty. 2020. Immunological memory to SARS-CoV-2
391 assessed for greater than six months after infection. *bioRxiv* 2020.2011.2015.383323.
392 Falck-Jones, S., S. Vangeti, M. Yu, R. Falck-Jones, A. Cagigi, I. Badolati, B. Osterberg, M.J.
393 Lautenbach, E. Ahlberg, A. Lin, I. Szurgot, K. Lenart, F. Hellgren, J. Salde, J. Albert, N.
394 Johansson, M. Bell, K. Lore, A. Farnert, and A. Smed-Sorensen. 2020. Functional
395 myeloid-derived suppressor cells expand in blood but not airways of COVID-19
396 patients and predict disease severity. *medRxiv*
397 Gaebler, C., Z. Wang, J.C.C. Lorenzi, F. Muecksch, S. Finkin, M. Tokuyama, M. Ladinsky, A.
398 Cho, M. Jankovic, D. Schaefer-Babajew, T.Y. Oliveira, M. Cipolla, C. Viant, C.O. Barnes,
399 A. Hurley, M. Turroja, K. Gordon, K.G. Millard, V. Ramos, F. Schmidt, Y. Weisblum, D.
400 Jha, M. Tankelevich, J. Yee, I. Shimeliovich, D.F. Robbiani, Z. Zhao, A. Gazumyan, T.
401 Hatziioannou, P.J. Bjorkman, S. Mehandru, P.D. Bieniasz, M. Caskey, and M.C.
402 Nussenzweig. 2020. Evolution of Antibody Immunity to SARS-CoV-2. *bioRxiv*
403 Grifoni, A., D. Weiskopf, S.I. Ramirez, J. Mateus, J.M. Dan, C.R. Moderbacher, S.A. Rawlings,
404 A. Sutherland, L. Premkumar, R.S. Jadi, D. Marrama, A.M. de Silva, A. Frazier, A.F.
405 Carlin, J.A. Greenbaum, B. Peters, F. Krammer, D.M. Smith, S. Crotty, and A. Sette.
406 2020. Targets of T Cell Responses to SARS-CoV-2 Coronavirus in Humans with COVID-
407 19 Disease and Unexposed Individuals. *Cell* 181:1489-1501 e1415.
408 Grissom, C.K., S.M. Brown, K.G. Kuttler, J.P. Boltax, J. Jones, A.R. Jephson, and J.F. Orme, Jr.
409 2010. A modified sequential organ failure assessment score for critical care triage.
410 *Disaster Med Public Health Prep* 4:277-284.
411 Gudbjartsson, D.F., G.L. Norddahl, P. Melsted, K. Gunnarsdottir, H. Holm, E. Eythorsson, A.O.
412 Arnthorsson, D. Helgason, K. Bjarnadottir, R.F. Ingvarsson, B. Thorsteinsdottir, S.
413 Kristjansdottir, K. Birgisdottir, A.M. Kristinsdottir, M.I. Sigurdsson, G.A. Arnadottir,
414 E.V. Ivarsdottir, M. Andresdottir, F. Jonsson, A.B. Agustsdottir, J. Berglund, B.
415 Eiriksdottir, R. Fridriksdottir, E.E. Gardarsdottir, M. Gottfredsson, O.S. Gretarsdottir,
416 S. Gudmundsdottir, K.R. Gudmundsson, T.R. Gunnarsdottir, A. Gylfason, A. Helgason,
417 B.O. Jensson, A. Jonasdottir, H. Jonsson, T. Kristjansson, K.G. Kristinsson, D.N.
418 Magnusdottir, O.T. Magnusson, L.B. Olafsdottir, S. Rognvaldsson, L. le Roux, G.

Sigmundsdottir, A. Sigurdsson, G. Sveinbjornsson, K.E. Sveinsdottir, M. Sveinsdottir, E.A. Thorarensen, B. Thorbjornsson, M. Thordardottir, J. Saemundsdottir, S.H. Kristjansson, K.S. Josefsdottir, G. Masson, G. Georgsson, M. Kristjansson, A. Moller, R. Palsson, T. Gudnason, U. Thorsteinsdottir, I. Jonsdottir, P. Sulem, and K. Stefansson. 2020. Humoral Immune Response to SARS-CoV-2 in Iceland. *N Engl J Med* 383:1724-1734.

Guthmiller, J.J., O. Stovicek, J. Wang, S. Changrob, L. Li, P. Halfmann, N.Y. Zheng, H. Utset, C.T. Stamper, H.L. Dugan, W.D. Miller, M. Huang, Y.N. Dai, C.A. Nelson, P.D. Hall, M. Jansen, K. Shanmugarajah, J.S. Donington, F. Krammer, D. Fremont, A. Joachimiak, Y. Kawaoka, V. Tesic, M.L. Madariaga, and P.C. Wilson. 2020. SARS-CoV-2 infection severity is linked to superior humoral immunity against the spike. *bioRxiv*

Hansen, C.B., I. Jarlhelt, L. Perez-Alos, L. Hummelshoj Landsy, M. Loftager, A. Rosbjerg, C. Helgstrand, J.R. Bjelke, T. Egebjerg, J.G. Jardine, C. Svaerke Jorgensen, K. Iversen, R. Bayarri-Olmos, P. Garred, and M.O. Skjoedt. 2020. SARS-CoV-2 Antibody Responses Are Correlated to Disease Severity in COVID-19 Convalescent Individuals. *J Immunol*

Intensivvårdsregistret, S. 2018. SIR:s riktlinje för registrering av SOFA. . In.

Isho, B., K.T. Abe, M. Zuo, A.J. Jamal, B. Rathod, J.H. Wang, Z. Li, G. Chao, O.L. Rojas, Y.M. Bang, A. Pu, N. Christie-Holmes, C. Gervais, D. Ceccarelli, P. Samavarchi-Tehrani, F. Guvenc, P. Budylowski, A. Li, A. Paterson, F.Y. Yue, L.M. Marin, L. Caldwell, J.L. Wrana, K. Colwill, F. Sicheri, S. Mubareka, S.D. Gray-Owen, S.J. Drews, W.L. Siqueira, M. Barrios-Rodiles, M. Ostrowski, J.M. Rini, Y. Durocher, A.J. McGeer, J.L. Gommerman, and A.C. Gingras. 2020. Persistence of serum and saliva antibody responses to SARS-CoV-2 spike antigens in COVID-19 patients. *Sci Immunol* 5:

Juno, J.A., H.X. Tan, W.S. Lee, A. Reynaldi, H.G. Kelly, K. Wragg, R. Esterbauer, H.E. Kent, C.J. Batten, F.L. Mordant, N.A. Gherardin, P. Pymm, M.H. Dietrich, N.E. Scott, W.H. Tham, D.I. Godfrey, K. Subbarao, M.P. Davenport, S.J. Kent, and A.K. Wheatley. 2020. Humoral and circulating follicular helper T cell responses in recovered patients with COVID-19. *Nat Med*

Lynch, K.L., J.D. Whitman, N.P. Lacanienta, E.W. Beckerdite, S.A. Kastner, B.R. Shy, G.M. Goldgof, A.G. Levine, S.P. Bapat, S.L. Stramer, J.H. Esensten, A.W. Hightower, C. Bern, and A.H.B. Wu. 2020. Magnitude and kinetics of anti-SARS-CoV-2 antibody responses and their relationship to disease severity. *Clin Infect Dis*

Moghadas, S.M., M.C. Fitzpatrick, P. Sah, A. Pandey, A. Shoukat, B.H. Singer, and A.P. Galvani. 2020. The implications of silent transmission for the control of COVID-19 outbreaks. *Proc Natl Acad Sci U S A*

Piccoli, L., Y.J. Park, M.A. Tortorici, N. Czudnochowski, A.C. Walls, M. Beltramello, C. Silacci-Fregni, D. Pinto, L.E. Rosen, J.E. Bowen, O.J. Acton, S. Jaconi, B. Guarino, A. Minola, F. Zatta, N. Sprugasci, J. Bassi, A. Peter, A. De Marco, J.C. Nix, F. Mele, S. Jovic, B.F. Rodriguez, S.V. Gupta, F. Jin, G. Piumatti, G. Lo Presti, A.F. Pellanda, M. Biggiogero, M. Tarkowski, M.S. Pizzuto, E. Cameroni, C. Havenar-Daughton, M. Smithey, D. Hong, V. Lepori, E. Albanese, A. Ceschi, E. Bernasconi, L. Elzi, P. Ferrari, C. Garzoni, A. Riva, G. Snell, F. Sallusto, K. Fink, H.W. Virgin, A. Lanzavecchia, D. Corti, and D. Veesler. 2020. Mapping Neutralizing and Immunodominant Sites on the SARS-CoV-2 Spike Receptor-Binding Domain by Structure-Guided High-Resolution Serology. *Cell*

Robbiani, D.F., C. Gaebler, F. Muecksch, J.C.C. Lorenzi, Z. Wang, A. Cho, M. Agudelo, C.O. Barnes, A. Gazumyan, S. Finkin, T. Hagglof, T.Y. Oliveira, C. Viant, A. Hurley, H.H. Hoffmann, K.G. Millard, R.G. Kost, M. Cipolla, K. Gordon, F. Bianchini, S.T. Chen, V.

Ramos, R. Patel, J. Dizon, I. Shimeliovich, P. Mendoza, H. Hartweger, L. Nogueira, M. Pack, J. Horowitz, F. Schmidt, Y. Weisblum, E. Michailidis, A.W. Ashbrook, E. Waltari, J.E. Pak, K.E. Huey-Tubman, N. Koranda, P.R. Hoffman, A.P. West, Jr., C.M. Rice, T. Hatziioannou, P.J. Bjorkman, P.D. Bieniasz, M. Caskey, and M.C. Nussenzweig. 2020. Convergent antibody responses to SARS-CoV-2 in convalescent individuals. *Nature*

Rodda, L.B., J. Netland, L. Shehata, K.B. Pruner, P.M. Morawski, C. Thouvenel, K.K. Takehara, J. Eggenberger, E.A. Hemann, H.R. Waterman, M.L. Fahning, Y. Chen, J. Rathe, C. Stokes, S. Wrenn, B. Fiala, L.P. Carter, J.A. Hamerman, N.P. King, M. Gale, D.J. Campbell, D. Rawlings, and M. Pepper. 2020. Functional SARS-CoV-2-specific immune memory persists after mild COVID-19. *medRxiv*

Rydyznski Moderbacher, C., S.I. Ramirez, J.M. Dan, A. Grifoni, K.M. Hastie, D. Weiskopf, S. Belanger, R.K. Abbott, C. Kim, J. Choi, Y. Kato, E.G. Crotty, C. Kim, S.A. Rawlings, J. Mateus, L.P.V. Tse, A. Frazier, R. Baric, B. Peters, J. Greenbaum, E. Ollmann Saphire, D.M. Smith, A. Sette, and S. Crotty. 2020. Antigen-Specific Adaptive Immunity to SARS-CoV-2 in Acute COVID-19 and Associations with Age and Disease Severity. *Cell*

Song, G., W.T. He, S. Callaghan, F. Anzanello, D. Huang, J. Ricketts, J.L. Torres, N. Beutler, L. Peng, S. Vargas, J. Cassell, M. Parren, L. Yang, C. Ignacio, D.M. Smith, J.E. Voss, D. Nemazee, A.B. Ward, T. Rogers, D.R. Burton, and R. Andrabi. 2020. Cross-reactive serum and memory B cell responses to spike protein in SARS-CoV-2 and endemic coronavirus infection. *bioRxiv*

Staines, H.M., D.E. Kirwan, D.J. Clark, E.R. Adams, Y. Augustin, R.L. Byrne, M. Cocozza, A.I. Cubas-Atienza, L.E. Cuevas, M. Cusinato, B.M.O. Davies, M. Davis, P. Davis, A. Duvoix, N.M. Eckersley, D. Forton, A. Fraser, G. Garrod, L. Hadcocks, Q. Hu, M. Johnson, G.A. Kay, K. Klekotko, Z. Lewis, J. Mensah-Kane, S. Menzies, I. Monahan, C. Moore, G. Nebe-von-Caron, S.I. Owen, C. Sainter, A.A. Sall, J. Schouten, C. Williams, J. Wilkins, K. Woolston, J.R.A. Fitchett, S. Krishna, and T. Planche. 2020. Dynamics of IgG seroconversion and pathophysiology of COVID-19 infections. *medRxiv*

Sterlin, D., A. Mathian, M. Miyara, A. Mohr, F. Anna, L. Claer, P. Quentric, J. Fadlallah, P. Ghillani, C. Gunn, R. Hockett, S. Mudumba, A. Guihot, C.-E. Luyt, J. Mayaux, A. Beurton, S. Fourati, J.-M. Lacorte, H. Yssel, C. Parizot, K. Dorgham, P. Charneau, Z. Amoura, and G. Gorochov. 2020. IgA dominates the early neutralizing antibody response to SARS-CoV-2. *medRxiv*

Vincent, J.L., R. Moreno, J. Takala, S. Willatts, A. De Mendonça, H. Bruining, C.K. Reinhart, P.M. Suter, and L.G. Thijs. 1996. The SOFA (Sepsis-related Organ Failure Assessment) score to describe organ dysfunction/failure. On behalf of the Working Group on Sepsis-Related Problems of the European Society of Intensive Care Medicine. *Intensive Care Med* 22:707-710.

Walls, A.C., Y.J. Park, M.A. Tortorici, A. Wall, A.T. McGuire, and D. Veesler. 2020. Structure, Function, and Antigenicity of the SARS-CoV-2 Spike Glycoprotein. *Cell* 181:281-292 e286.

Wrapp, D., N. Wang, K.S. Corbett, J.A. Goldsmith, C.L. Hsieh, O. Abiona, B.S. Graham, and J.S. McLellan. 2020. Cryo-EM structure of the 2019-nCoV spike in the prefusion conformation. *Science* 367:1260-1263.

Zaki, N., H. Alashwal, and S. Ibrahim. 2020. Association of hypertension, diabetes, stroke, cancer, kidney disease, and high-cholesterol with COVID-19 disease severity and fatality: A systematic review. *Diabetes Metab Syndr* 14:1133-1142.

Zhao, J., Q. Yuan, H. Wang, W. Liu, X. Liao, Y. Su, X. Wang, J. Yuan, T. Li, J. Li, S. Qian, C. Hong, F. Wang, Y. Liu, Z. Wang, Q. He, Z. Li, B. He, T. Zhang, Y. Fu, S. Ge, L. Liu, J. Zhang, N. Xia, and Z. Zhang. 2020. Antibody Responses to SARS-CoV-2 in Patients With Novel Coronavirus Disease 2019. *Clin Infect Dis* 71:2027-2034.

Zielinski, C.E., D. Corti, F. Mele, D. Pinto, A. Lanzavecchia, and F. Sallusto. 2011. Dissecting the human immunologic memory for pathogens. *Immunol Rev* 240:40-51.

Figure legends

Figure 1. Study and sampling overview. A) Overview of study cohort and controls, timeline of longitudinal sampling, the anatomical compartments analyzed, and the measurements performed. AS=asymptomatic. **(B)** Patient sampling overview with first study sample (color) and first convalescent sample (open) indicated for each patient, hospital admission/discharge, level of care and outcome. Patients are group based on peak disease severity (PDS); mild (PDS 1 and 2), moderate (PDS 3 and 4), severe (PDS 5 and 6) and fatal (PDS 7). Individual inclusion sample for each patient is color-coded based on disease severity at the time of sampling.

Figure 2. Plasma IgG and IgA responses to N, S and RBD across COVID-19 severity during acute disease and convalescence. A) Individual levels of plasma IgG and IgA (from left to right) in SARS-CoV-2 infected individuals with different peak disease severity (PDS). Data in cyan and green refer to mild disease (PDS 1 and 2), yellow and orange refer to moderate disease (PDS 3 and 4), red and cayenne refer to severe disease (PDS 5 and 6) and grey refers to patients with fatal outcome (PDS 7). Black lines indicate medians and dotted lines indicate the average background level from pre-pandemic healthy controls. Mann-Whitney U was used to compare the groups and considered statistically significant at $p<0.05$. ** $p<0.01$, *** $p<0.001$, **** $p<0.0001$. **B)** Spearman correlation for plasma IgG (top) and IgA (bottom) against the RBD versus days from onset of symptoms during the acute and the convalescent phases are shown. Circles with black lining refer to convalescent samples. **C-D)** Longitudinal measurements of plasma IgG against RBD on a subset of patients with moderate/severe disease and fatal outcome who had low (< 1.0 OD) antibody titers at the time of study inclusion and were longitudinal samples from symptomatic (acute) disease were available. Levels are shown at the time of study inclusion, during the late acute phase and at convalescence, and shown with respect to days from onset of symptoms and as a group comparison. The black lines connect data points from the same individuals. Wilcoxon test was used to compare the groups separately and considered statistically significant at $p<0.05$. **** $p<0.0001$.

Figure 3. Airway IgG and IgA responses to RBD across COVID-19 severity during acute disease and convalescence. A) Levels of IgG and IgA to RBD in nostrils swabs (NSW) and nasopharyngeal aspirates (NPA). The black lines indicate median values. Mann-Whitney U was used to compare the group and considered statistically significant at $p<0.05$. *$p<0.05$ ** $p<0.01$, *** $p<0.001$, **** $p<0.0001$. **B)** Heat map generated grouping patients according to PDS showing acute and convalescent IgG and IgA titers against N, S and RBD (plasma) and RBC (NSW, NPA and ETA) for each patient. The heat map also includes data from PPHC and PCR-individuals (indicated with PDS 0). Missing data and not available samples are shown in

black. **C)** Spearman correlation for NPA versus plasma immunoglobulins against the RBD during acute disease. In A) the line overlaps with not detected (ND) for IgG levels. **D)** Comparison of the levels of RBD IgG/A in patient-matched NSW, NPA, endotracheal aspirates (ETA) and plasma collected at the same time point. The black lines connect data points from the same individuals. Wilcoxon test was used to compare the groups separately and considered statistically significant at $p<0.05$. **** $p<0.0001$.

Figure 4. Assessment of frequencies of B cells in the respiratory tract and of circulating S-specific memory B cells. A) Representative example with gating strategy for the identification of lymphocytes (identified as negative for CD14/16/123/66) and of total B cells (CD3-CD19+) in respiratory NPA and ETA samples. **B)** Levels of lymphocytes and of total B cells in NPA and ETA in a subset of patients alongside with NPA from healthy controls. Mann-Whitney test was used to compare the groups and considered statistically significant at $p<0.05$. ** $p<0.01$.
C) Representative examples with gating strategy of SARS-Cov-2 S-specific memory B cells from one pre-pandemic healthy control, convalescent samples from one SARS-CoV-2 PCR-individual and one mild and one moderate/severe COVID-19 patient. Further characterization of S-positive memory B cells on RBD binding and B cell isotype (IgG+ or IgA+ assumed to correspond to IgD-IgM-IgG- B cells). **D)** Pie charts show the cumulative proportion of RBD binding and memory B cell isotypes in convalescent samples from mild (n=6) and moderate/severe (n=8) COVID-19 patients. **E)** Frequencies of S-specific memory B cells in matched acute (filled) and convalescent (filled with black lining) PBMCs in relation to days in the subset of individuals analyzed color-coded according to PDS. Dotted lines on indicate the average background staining from PCR- and PPHC. **F)** Levels of circulating Spike+ switched memory B cells during acute disease and convalesce in the subset of patients analyzed, as well as PPHC, color-coded according to PDS. Circles with black lining refer to data during the convalescent phase. Black triangles symbolize the PPHC. Differences were assessed using Kruskal -Wallis with Dunn's multiple comparisons test and considered statistically significant at $p<0.05$. ** $p<0.01$.

Table 1. Clinical characterization of the SARS-CoV-2 infected cohort.

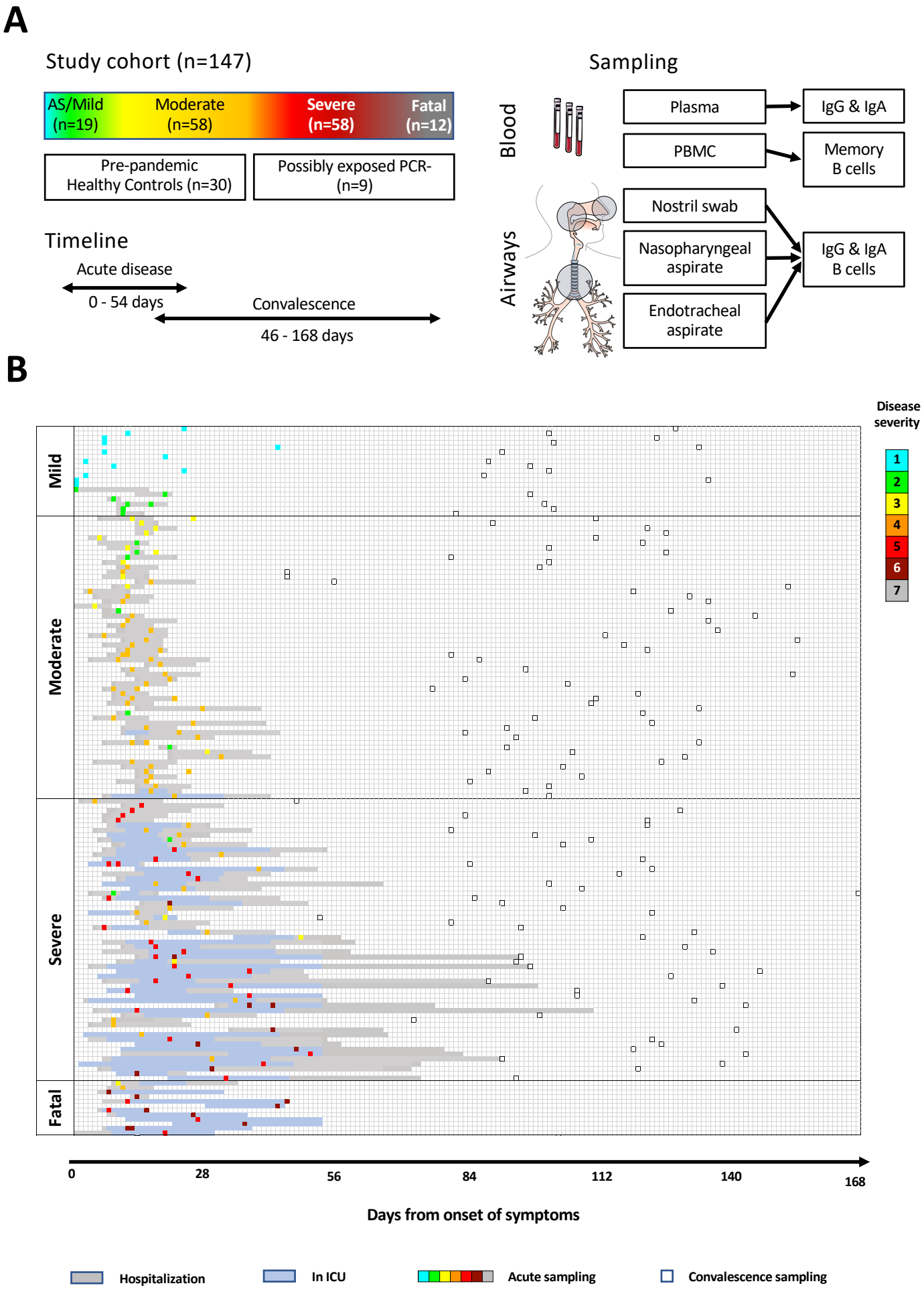

Figure 1

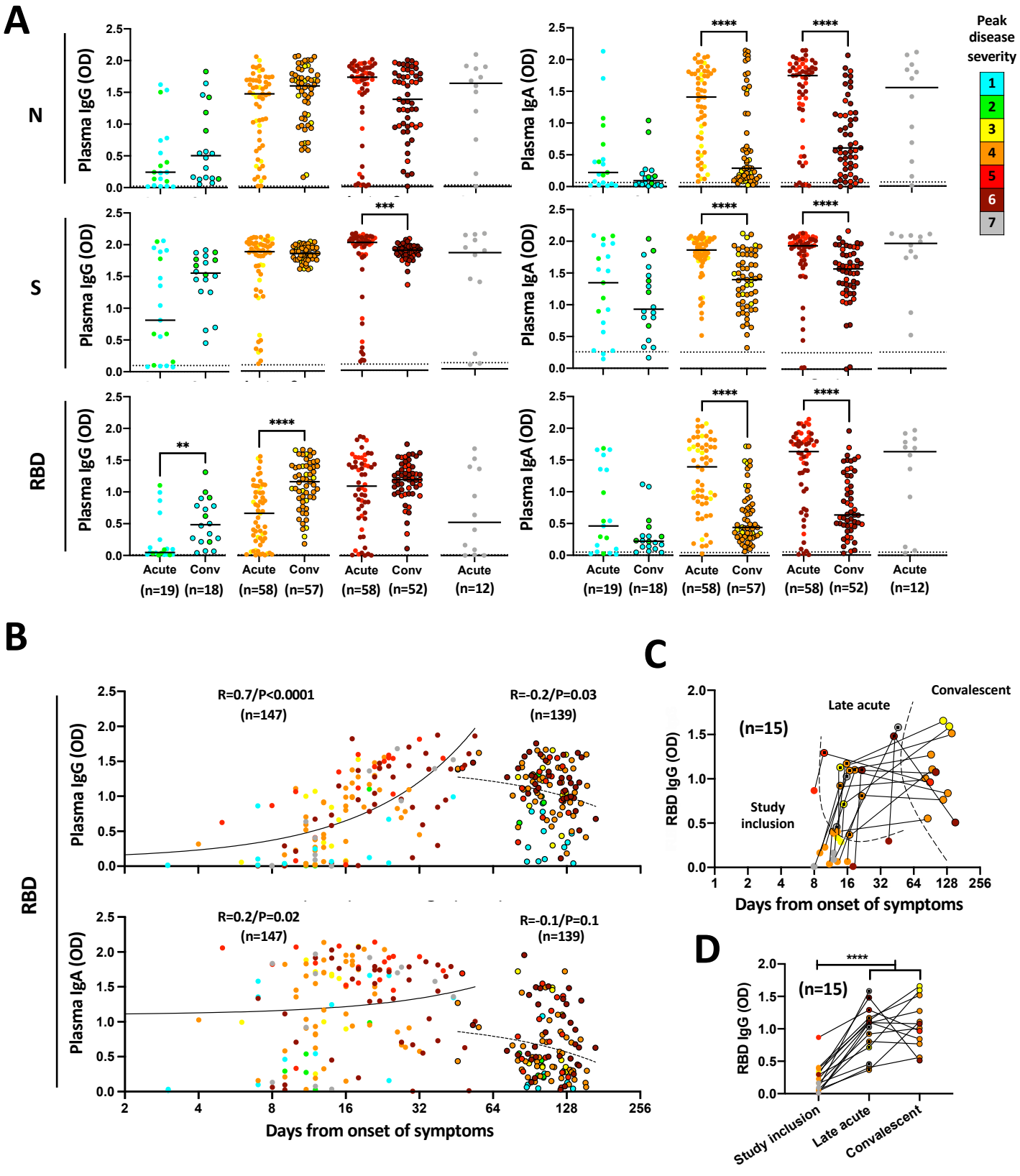
A
N
S
RBD
Plasma IgG (OD)
Plasma IgA (OD)
Peak disease severity
1
2
3
4
5
6
7
Acute (n=19)
Conv (n=18)
Acute (n=58)
Conv (n=57)
Acute (n=58)
Conv (n=52)
Acute (n=12)
B
RBD
R=0.7/P<0.0001 (n=147)
R=-0.2/P=0.03 (n=139)
R=0.2/P=0.02 (n=147)
R=-0.1/P=0.1 (n=139)
Days from onset of symptoms
C
RBD IgG (OD)
(n=15)
Late acute
Convalescent
Study inclusion
Days from onset of symptoms
D
RBD IgG (OD)
(n=15)
Study inclusion
Late acute
Convalescent

Figure 2

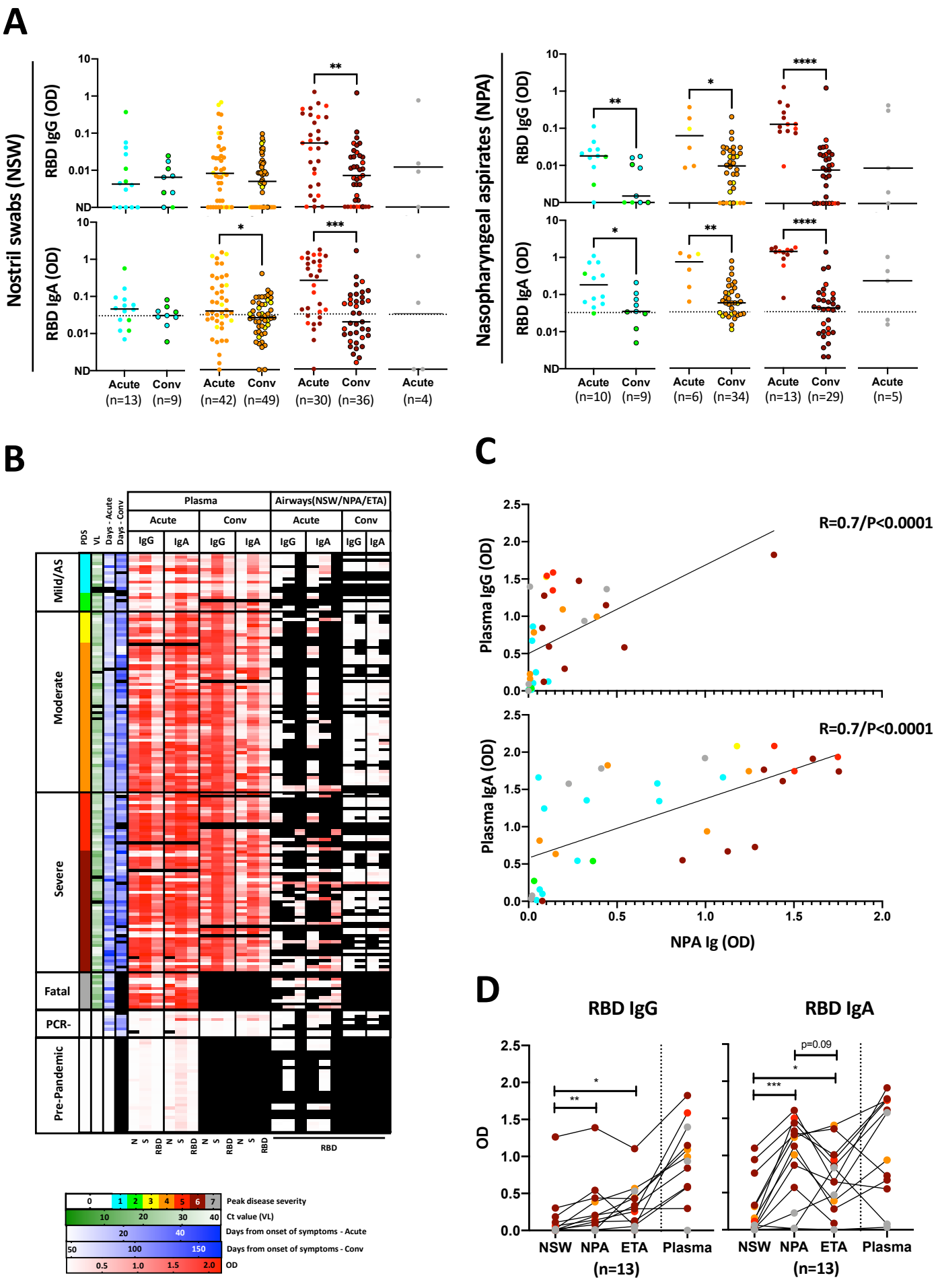
A
Nostril swabs (NSW)
RBD IgG (OD)
RBD IgA (OD)
Nasopharyngeal aspirates (NPA)
Acute (n=13)
Conv (n=9)
Acute (n=42)
Conv (n=49)
Acute (n=30)
Conv (n=36)
Acute (n=4)
Acute (n=10)
Conv (n=9)
Acute (n=6)
Conv (n=34)
Acute (n=13)
Conv (n=29)
Acute (n=5)
B
Plasma
Airways(NSW/NPA/ETA)
Acute
Conv
IgG
IgA
PDS
VL
Days - Acute
Days - Conv
Mild/AS
Moderate
Severe
Fatal
PCR-
Pre-Pandemic
N
S
RBD
Peak disease severity
Ct value (VL)
Days from onset of symptoms - Acute
Days from onset of symptoms - Conv
OD
C
R=0.7/P<0.0001
Plasma IgG (OD)
Plasma IgA (OD)
NPA Ig (OD)
D
RBD IgG
RBD IgA
OD
p=0.09
NSW
NPA
ETA
Plasma
(n=13)

Figure 3

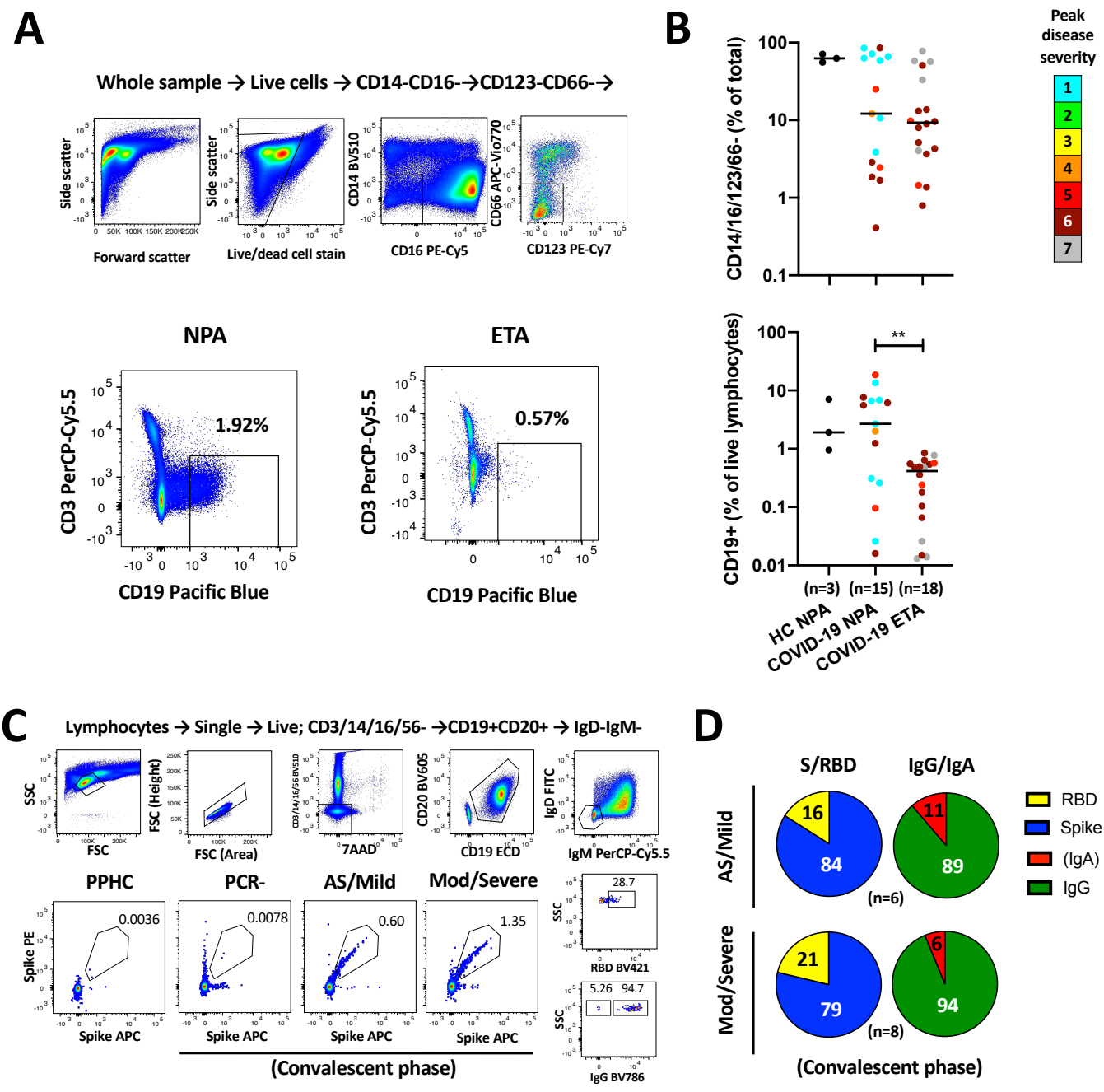
A
Whole sample → Live cells → CD14-CD16-→CD123-CD66-→
Side scatter
Forward scatter
Side scatter
Live/dead cell stain
CD14 BV510
CD16 PE-Cy5
CD66 APC-Vio770
CD123 PE-Cy7
NPA
ETA
CD3 PerCP-Cy5.5
1.92%
CD19 Pacific Blue
CD3 PerCP-Cy5.5
0.57%
CD19 Pacific Blue
B
CD14/16/123/66- (% of total)
Peak disease severity
1
2
3
4
5
6
7
CD19+ (% of live lymphocytes)
**
(n=3) (n=15) (n=18)
HC NPA
COVID-19 NPA
COVID-19 ETA
C
Lymphocytes → Single → Live; CD3/14/16/56- →CD19+CD20+ → IgD-IgM-
SSC
FSC
FSC (Height)
FSC (Area)
7AAD
CD20 BV605
CD19 ECD
IgD FITC
IgM PerCP-Cy5.5
PPHC
PCR-
AS/Mild
Mod/Severe
Spike PE
0.0036
0.0078
0.60
1.35
Spike APC
28.7
RBD BV421
5.26 94.7
IgG BV786
(Convalescent phase)
D
S/RBD
IgG/IgA
AS/Mild
16
84
11
89
(n=6)
Mod/Severe
21
79
6
94
(n=8)
RBD
Spike
(IgA)
IgG
(Convalescent phase)
E
Spike+ switched memory B cells
% of CD19/20+ IgD/M-
ND
PCR- (n=6)
PPHC (n=6)
Days from onset of symptoms
F
Spike+ switched memory B cells
**
**
% of CD19/20+ IgD/M-
ND
Peak disease severity
1 (n=6)
4 (n=5)
5 (n=1)
6 (n=2)
(n=6) (n=6) (n=8)
PPHC
AS/Mild (Acute)
AS/Mild (Conv)
Mod/Severe (Acute)
Mod/Severe (Conv)

Figure 4

Table 1. Clinical characterization of the SARS-CoV-2 infected cohort.

Disease severity	Mild		Moderate		Severe		Fatal
PDS	1	2	3	4	5*	6*	7
Resp. SOFA score	0	0	1	2	3	4	
Admitted (Y/N)	N	Y	Y	Y	Y	Y	Y
PFI (kPa) SFI	> 53 > 400	> 53 > 400	< 53 ≤ 400	< 40 ≤ 315	< 27 ≤ 235	< 13 < 150	-
Number of individuals (%)	13 (8.8)	6 (4.1)	10 (6.8)	48 (33)	19 (13)	39 (27)	12 (8.2)
Age, mean (Range)	44 (24-72)	60 (41-72)	56 (46-78)	55 (24-76)	57 (42-74)	61 (25-77)	66 (52-78)
Male (%)	5 (38)	2 (33)	6 (60)	38 (79)	15 (79)	34 (87)	9 (75)
Days from symptoms to admission – median (Range)	-	10 (0-14)	8.5 (4-14)	10 (3-21)	7 (2-14)	10 (2-35)	7 (1-28)
Days from symptoms to inclusion “Acute” – median (Range)	9 (3-44)	11 (0-20)	13.5 (6-18)	13 (4-32)	21 (5-40)	22 (7-54)	13 (8-44)
Days from symptoms to follow-up “Conv” – median (Range)	102 (88-136)	99,5 (82-103)	112 (81-127)	109 (46-155)	109 (48-130)	120 (53-168)	-
VL (Ct value) median (Range)	27.5 (40-14)	25.0 (29-14)	26.7 (36-15)	26.8 (36-12)	25.8 (36-19)	24.0 (37-14)	20.5 (32-13)
CCI, mean (SD)	1 (2)	2 (1)	1 (1)	2 (2)	2 (1)	2 (1)	3 (1)
BMI, mean (SD)	24.1 (4.5)	25.1 (2.2)	26.0 (3.2)	30.3 (4.2)	29.2 (5.3)	28.6 (4.7)	28.6 (2.4)
Hypertension (%)	1 (8.3)	0 (0)	2 (20)	20 (42)	8 (42)	15 (38)	9 (75)
Diabetes (%)	2 (17)	0 (0)	1 (10)	14 (29)	5 (26)	9 (23)	3 (25)
Current smokers (%)	0 (0)	0 (0)	2 (20)	5 (11)	1 (5.3)	2 (5.3)	0 (0)
ACE-I (%)	0 (0)	0 (0)	0 (0)	5 (10)	1 (5.3)	4 (10)	1 (9.1)
IS drugs (%)	1 (7.7)	0 (0)	0 (0)	4 (8.3)	2 (11)	5 (13)	1 (8.3)

PDS: Peak Disease Severity
SOFA: Sequential Organ Failure Assessment
PFI: PaO_2/FiO_2-index
SFI: SpO_2/FiO_2-index
VL: Viral Load
CCI: Charlson comorbidity index
BMI: body mass index
ACE-I: angiotensin converting enzyme-inhibitors
IS: immunosuppressive
*Requires mechanical ventilation